

pubs.acs.org/acschemicalbiology Articles

R-BIND 2.0: An Updated Database of Bioactive RNA-Targeting Small Molecules and Associated RNA Secondary Structures

Anita Donlic, Emily G. Swanson, Liang-Yuan Chiu, Sarah L. Wicks, Aline Umuhire Juru, Zhengguo Cai, Kamillah Kassam, Chris Laudeman, Bilva G. Sanaba, Andrew Sugarman, Eunseong Han, Blanton S. Tolbert, and Amanda E. Hargrove



Cite This: https://doi.org/10.1021/acschembio.2c00224



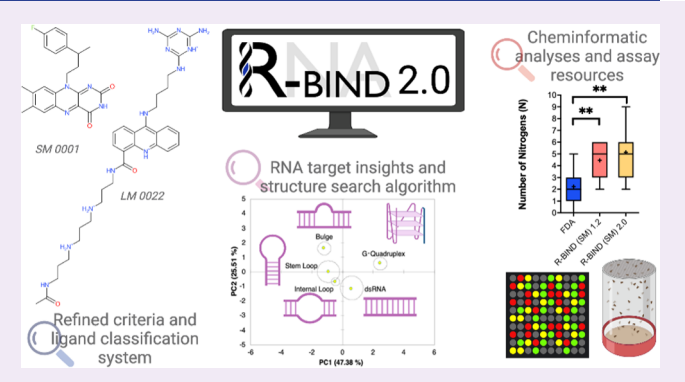
ACCESS

III Metrics & More

Article Recommendations

s Supporting Information

ABSTRACT: Discoveries of RNA roles in cellular physiology and pathology are increasing the need for new tools that modulate the structure and function of these biomolecules, and small molecules are proving useful. In 2017, we curated the RNA-targeted BIoactive ligaNd Database (R-BIND) and discovered distinguishing physicochemical properties of RNA-targeting ligands, leading us to propose the existence of an "RNA-privileged" chemical space. Biennial updates of the database and the establishment of a website platform (rbind.chem.duke.edu) have provided new insights and tools to design small molecules based on the analyzed physicochemical and spatial properties. In this report and R-BIND 2.0 update, we refined the curation approach and ligand classification system as well as conducted analyses of RNA



structure elements for the first time to identify new targeting strategies. Specifically, we curated and analyzed RNA target structural motifs to determine the properties of small molecules that may confer selectivity for distinct RNA secondary and tertiary structures. Additionally, we collected sequences of target structures and incorporated an RNA structure search algorithm into the website that outputs small molecules targeting similar motifs without a priori secondary structure knowledge. Cheminformatic analyses revealed that, despite the 50% increase in small molecule library size, the distinguishing properties of R-BIND ligands remained significantly different from that of proteins and are therefore still relevant to RNA-targeted probe discovery. Combined, we expect these novel insights and website features to enable the rational design of RNA-targeted ligands and to serve as a resource and inspiration for a variety of scientists interested in RNA targeting.

INTRODUCTION

RNA molecules are being recognized as major modulators and therapeutic targets in human diseases ranging from cancer, neurodegenerative,² and cardiovascular³ diseases as well as viral, bacterial, and fungal infections. As a consequence, small molecule-based targeting of RNA is gaining increased attention in academia and industry, exemplified by the increasing number of publications with RNA-targeting bioactive ligands (Figure 1A).^{7–13} Recent years serve as both proof and inspiration of the vast potential for successful RNA targeting in the clinic, as shown by the FDA approval of risdiplam for spinal muscular atrophy in August 2020. 14 This success represents the first drug targeting a nonribosomal RNA molecule and thus reminds the community that many unanswered questions remain in the field. Additionally, the growing number of known noncoding RNA functions in various biological systems increases the need for new chemical probes to spatiotemporally investigate the cellular processes regulated by these biomolecules.¹⁵

A long-standing hypothesis in the field is that progress toward RNA-targeted probe and drug discovery is hindered by our lack

of understanding of the nature of RNA-small molecule interactions, which may be different from those of proteins. Toward elucidating these fundamental principles, our laboratory curated the first database of nonribosomal RNA-binding ligands to include bioactivity as a criterion for inclusion in 2017, termed the RNA-targeted BIoactive ligaNd Database (R-BIND). Its analyses and updates led to the first quantitative comparison and discovery of distinguishing the properties of RNA-binding molecules that are different from those of protein-targeting ligands. If, The existence of this "RNA-privileged chemical space" has been supported by other recent work in the field. For example, similar physicochemical properties were found to be increased in hits in large RNA-targeted screens.

Received: March 14, 2022 Accepted: May 3, 2022



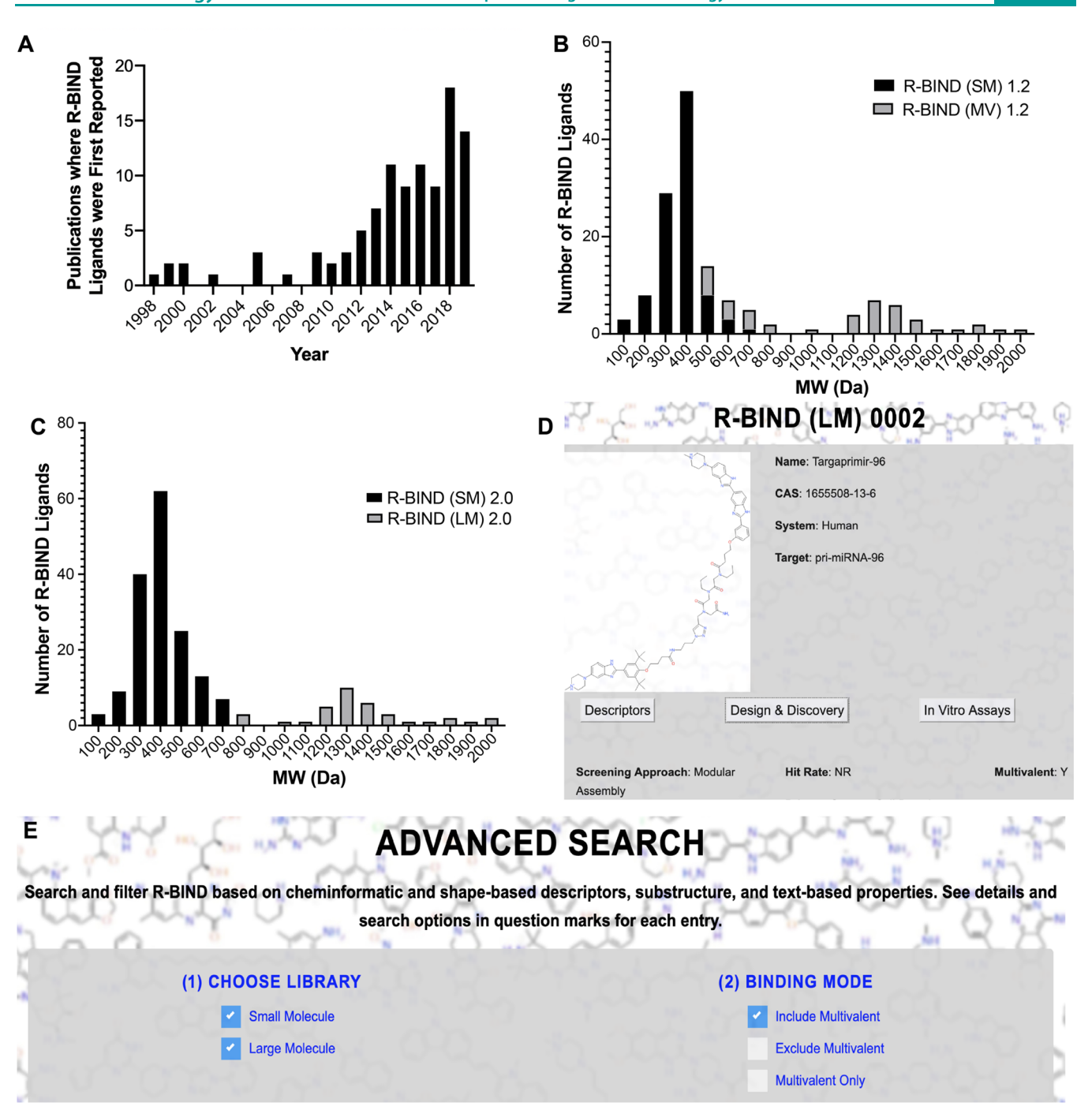


Figure 1. Reclassification of database ligands based on molecular weight (MW) and associated new search features. (A) Histogram of articles published reporting ligands that are included in the R-BIND database. (B) Histogram of R-BIND 1.2 classified by SM and MV. (C) Histogram of R-BIND 2.0 with new classifications of SM and LM. For histograms, each bin covers 100 Da and the center of the bin is the number listed on the *x*-axis. For example, bin "200" covers ligands with MW between 150 and 250 Da. (D) Website image of new screening approach "modular assembly" and "multivalent: Y" under the Design and Discovery tab in Single Molecule View. (E) Website image showing the ability to search using multivalency as a criterion under the "Advanced Search". SM, small molecule; MV, multivalent; LM, large molecule; and Y, Yes.

libraries with these properties led to a higher propensity for binding to RNA vs protein targets. ¹⁹ Furthermore, recent comprehensive analyses and comparisons of small molecule-bound RNA and protein complexes in the Protein Database (PDB) by Schneekloth and co-workers ²⁰ and Hargrove and co-workers ²¹ revealed differences in pocket properties and interaction types, respectively. The identification of more polar binding pockets in RNA along with the prevalence of stacking and hydrogen-bonding interactions in those pockets

further supports the significance of the enriched molecular recognition parameters identified in R-BIND ligands. Together, these reports corroborate the value of databases such as R-BIND to serve as a reliable resource for designing screening libraries with unique RNA-privileged properties and ultimately expediting the detection of novel probes and drugs.

To make this chemical space and information useful to the community, we recently reported a user-friendly website platform of the R-BIND database (rbind.chem.duke.edu) and

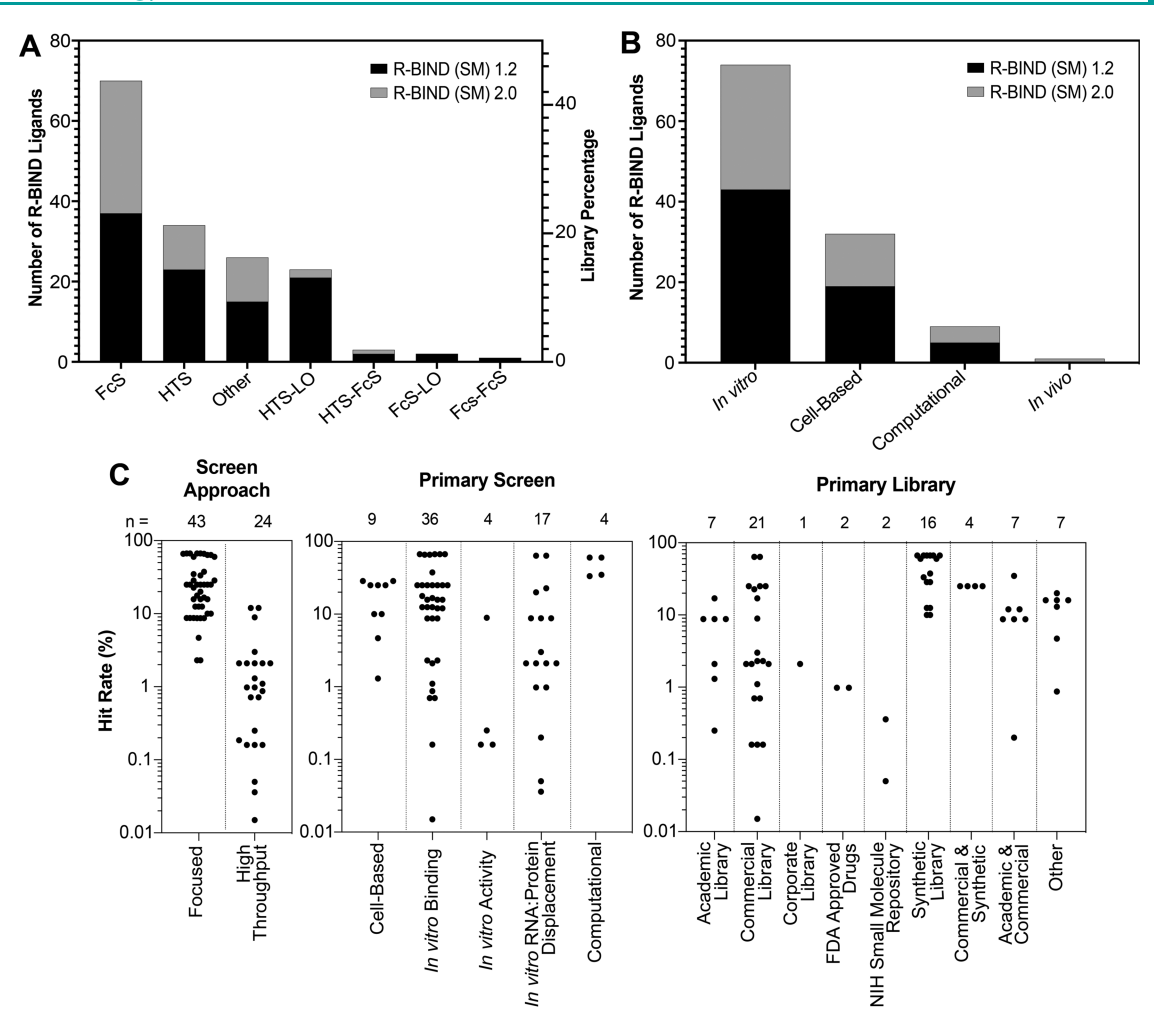


Figure 2. Analysis of screening libraries and approaches utilized in R-BIND (SM) 1.2 and 2.0. (A) Number of molecules discovered by various screening approaches by R-BIND (SM) 1.2 and 2.0. (B) Number of molecules discovered by primary screen methods in R-BIND (SM) 1.2 and 2.0. (C) Hit rates of screens by screening approach, primary screen method, and library source for R-BIND (SM) 2.0. FcS, focused screen; HTS, high-throughput screen; and LO, lead optimization.

offered a number of resources for a diverse community of researchers. For medicinal chemists, we provided tools to identify novel lead molecules for existing targets via structure-based searches and to design ligands in RNA-privileged space using a nearest-neighbor algorithm. For chemical, molecular, and cell biologists, we extensively curated qualitative information to efficiently select probes and methods for in vitro, cell, and animal experiments. Based on community feedback, and as supported by the established success of the structure-based rational design in targeting a variety of RNA structural elements, we envisioned R-BIND users further benefiting from the incorporation of an RNA secondary structure search tool in this update.

In R-BIND 2.0, we conducted an analysis of RNA structure—ligand pairs and identified features that may be privileged for binding particular structural elements. For the field to benefit from these novel insights, we incorporated a feature termed "RNA Structure Search". This algorithm uses an input RNA sequence or structure of interest, conducts an RNA structure prediction, and then returns ligands in the database that bind that motif (if any) based on secondary structure and size. We also collected follow-up studies for existing database ligands as well as new reports, which were published between June 1st, 2018 and December 31st, 2019 and found that, despite the small

molecule database ligand number increasing by 50% (n = 97 to n = 153), distinguishing cheminformatics and shape-based trends remained the same for R-BIND small molecule database members when compared to those for protein-targeting ligands. Moreover, we made changes in the ligand classification and website information display to more appropriately reflect the set of small molecules as well as highlight distinct strategies of RNAtargeted ligand design. R-BIND 2.0 is complementary to the Disney group's Inforna database, 25 which compiles data from an in-house two-dimensional combinatorial screen against a panel of RNA secondary structures and requires a priori knowledge of the structure or prediction from other prediction platforms. In contrast, R-BIND 2.0 compiles all literature-reported bioactive RNA ligands and their experimental information along with cheminformatic properties and RNA structure-based tools for the design and discovery of new ligands. Together, the R-BIND 2.0 update is unique compared to the previous 1.2 update in that it incorporates the analysis of RNA structure targets and an accompanying RNA structure search algorithm on the R-BIND website platform. Combined with the continued extensive cataloging of all experimental details from new reports and associated cheminformatics analyses of all new ligands, R-BIND 2.0 represents to date the most comprehensive set of tools and

insights to aid researchers interested in RNA recognition and drug discovery.

RESULTS

R-BIND 2.0 Update Includes Refined Criteria and Ligand Classification System. R-BIND ligand inclusion criteria are continuously refined and clarified with each update. In general, we consider chemical probes with molecular weight (MW) < 2000 Da that bind to nonribosomal RNA targets in vitro via noncovalent interactions and have demonstrated activity in cell culture and/or animal models. In this update, we expanded the explicit criteria to state that common nucleic acid intercalators were excluded unless the primary literature report provided experimental evidence that the biological phenotype observed was a result of RNA target binding. The new criteria are outlined in SI Section 1A and in the website "about" and "contribute" sections.

In addition, we implemented a nomenclature change and reclassification in two ligand libraries. Previously, ligands were separated into a "traditional" small molecule (SM) library (~500 Da) and a multivalent (MV) library. The latter contained larger MW ligands explicitly designed to bind RNA multivalently or those that resemble such ligands and were thus expected to occupy a distinct chemical space. The increased MW of MV library members was expected given their design strategies of combining RNA-binding moieties composed of "traditional" SMs interspaced with specific linkers. All previous cheminformatic analyses and comparisons to FDA-approved drugs were thus conducted with the (SM) library. Throughout previous curations and analyses of the two libraries, however, we noted that while the biggest difference between SM and MV ligands based on the physicochemical properties was the average molecular weight (MW), 16,17,22 there was overlap between the two libraries. An MW histogram of R-BIND (SM) 1.2 and R-BIND (MV) 1.2 illustrated that the SM ligands' MW ranged from 100 to 700 Da, while that of MV ranged from 500 to 2000 Da (Figure 1B).

We reasoned that the exclusion of low-MW MV ligands from the SM group solely based on their design strategy may lead to future biases in the chemical space for RNA-targeted small molecules, which would ideally be defined based on the cheminformatics properties and not design strategy. We thus decided to classify two libraries based on an MW cutoff, as defined by the largest MW bin in which an R-BIND (SM) 1.2 ligand is located (R-BIND (SM) 0069, MW = 665.91 Da, histogram bin = 700 Da as per Figure 1B). Ligands in R-BIND 2.0 were thus classified as follows: small molecules (SM, n =153) to encompass ligands in bins 700 Da and below, and large molecules (LM, n = 35) for those in bins larger than 700 Da (Figure 1C). To provide information on multivalent ligand design and keep those as searchable features on the website, a new column was added to the "Screening Approach" tab of the "Design and Discovery" section of both libraries to indicate multivalency and "modular assembly" was added as a new Screening Approach category for these ligands (Figure 1D,E). Together, the R-BIND 2.0 update resulted in a total number of 188 R-BIND members, a 25% increase in size compared to 1.2.

Update 2.0 Reveals Notable Screening Trends, Novel Targets, and Advances in Discovery Strategies. In addition to updating inclusion criteria, we utilize each R-BIND update to note new achievements and emerging strategies in the field. In terms of screening approaches, we observed a significant increase of ligands discovered via focused screens in

R-BIND (SM) 2.0 (57%), compared to 36% of the R-BIND (SM) 1.2 library (Figure 2A). In types of primary screens (Figure 2B), we noted the first in vivo primary screen in R-BIND 2.0, reported by Chan et al., in a patent application for DB213 against CAG repeats found in Huntington's disease.26 Specifically, a series of synthesized small molecules were screened in two Drosophila models for polyglutamine-repeat disease. Three compounds were shown to suppress neurodegeneration in a Machado-Joseph disease model and were then tested for CAG-repeat RNA-dependent toxicity in a transgenic Drosophila $DsRed_{CAG100}$ model. DB213 was shown to rescue the RNA-dependent toxicity in a dose-dependent manner, as revealed by a pseudopupil assay in this CAG expansion repeat model but not in control models. Except for this screen, most screens were initially performed in vitro rather than through cell-based or computational approaches, with bioactivity being assessed in follow-up experiments, consistent with previous updates (Figure 2B). In library types, we noted higher hit rates in focused and synthetic libraries (Figure 2C), which is also consistent with previously described trends. 17

We also noted increased diversity in targets and discovery strategies. Specifically, advances in long noncoding RNA (lncRNA) targeting were made, as seen by the first reports of bioactive binders for oncogenic MALAT1²⁷ (R-BIND (SM) 0113 and 0114) and HOTAIR²⁸ (R-BIND (SM) 0137) lncRNAs. Furthermore, an increase in traditionally underrepresented fungal RNA targets was observed with the discovery of first group II intron binders in Candida parapsilosis by Pyle and co-workers⁶ (R-BIND (SM) 0121 and 0122), and the first application of differential scanning fluorimetry as a high-throughput screen for pre-microRNA 21 inhibitors (R-BIND (SM) 0146, 0147 and 0148) was reported.²⁹

Important insights were gained from follow-up studies for previously identified R-BIND ligands, some of which included the addition of new derivatives with the same inferred mode of action. For example, a recent report that outlined structure—activity relationships of antibacterial riboflavin mononucleotide analogues (R-BIND SM 0001 and 0004) led to the addition of R-BIND (SM) 0149 to R-BIND 2.0.³⁰ Structural information for small molecule splicing modulators in spinal muscular atrophy determined by NMR (R-BIND (SM) 0095) provided significant insights into the mechanism of action for these ligands,³¹ highlighting the importance of allosteric modulation of RNA—protein complexes in diseases.

Cheminformatic Analyses Further Support the Existence of RNA-Privileged Chemical Space. R-BIND (SM) 1.2 vs 2.0. Cheminformatic analyses of R-BIND ligands have relied on calculating 20 standard physicochemical properties along with three-dimensional (3D) properties using principal moments of inertia (PMI) analysis. ¹⁶ With the addition of new ligands and reclassification of the database for the R-BIND 2.0 update, some of the library averages for the 20 parameters have shifted when compared to the previous (SM) 1.2 update (Table S4). First, an increase in the average molecular weight was observed with the latest update and found to be statistically significantly different as per the Mann-Whitney U analysis in the latest update (P-value = 0.02). As a consequence of the MW increase, increases in averages of other parameters were observed as well. For example, accessible surface area (ASA) was found to have a statistically significant increase in R-BIND (SM) 2.0 compared to that in R-BIND (SM) 1.2 (P-value = 0.03). To confirm that these changes were due to the new MWbased library classifications, we conducted a Mann-Whitney U

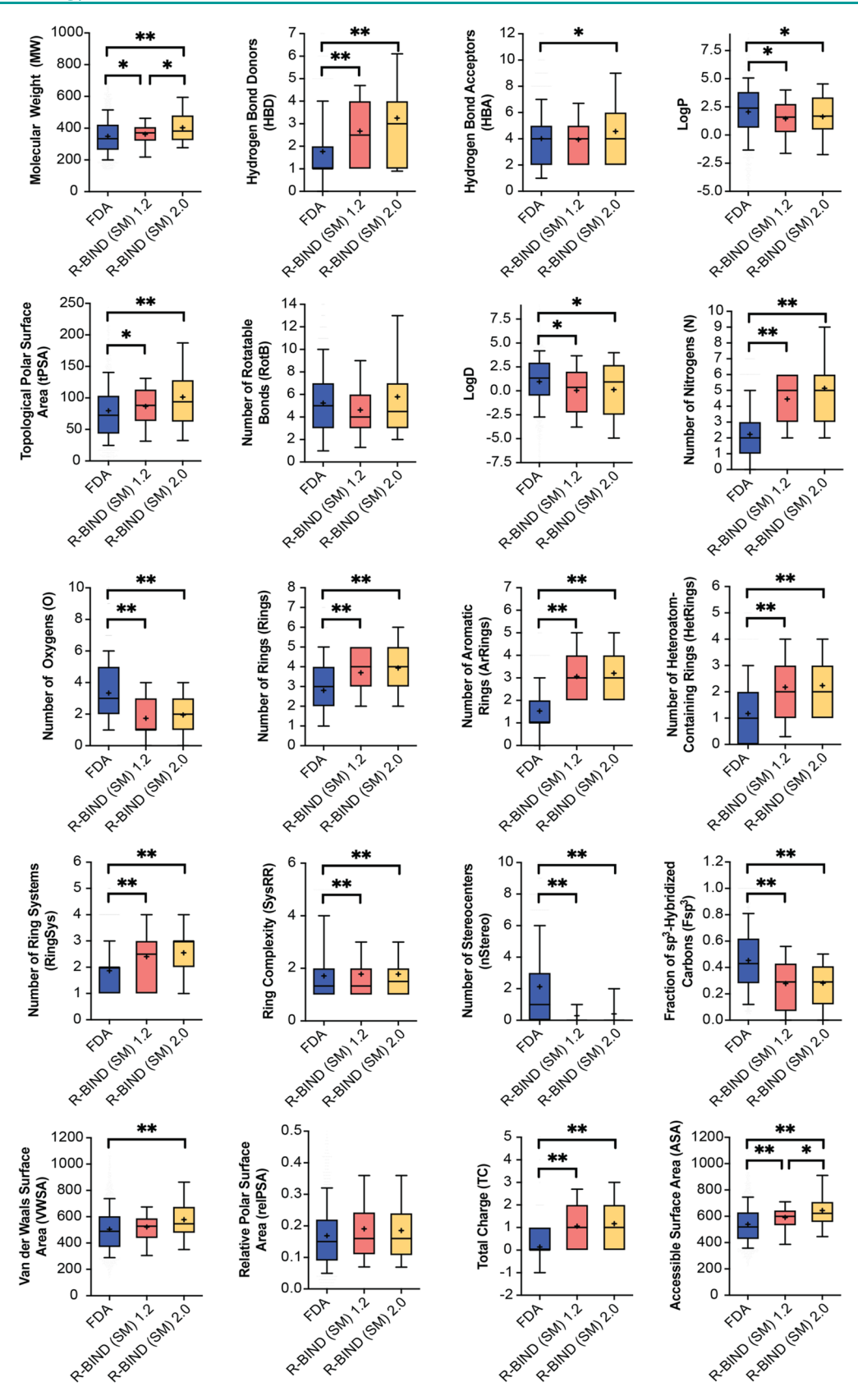


Figure 3. Statistical analysis of cheminformatic parameters between R-BIND (SM) 1.2 and 2.0 and the updated FDA library (MW-filtered). The box encompasses 25-75% of variance, while the whiskers describe 10-90%. The mean is indicated by the + symbol, and the line designates the median value. All comparisons are performed using the Mann–Whitney U test with statistically significant differences indicated as *P < 0.05 and **P < 0.001.

test, which showed that if the MW cutoff from R-BIND (SM) 1.2 is applied to the new set of molecules in the R-BIND (SM)

2.0 update, the MW and ASA are no longer significantly different (Table S5). We can thus conclude that these differences were

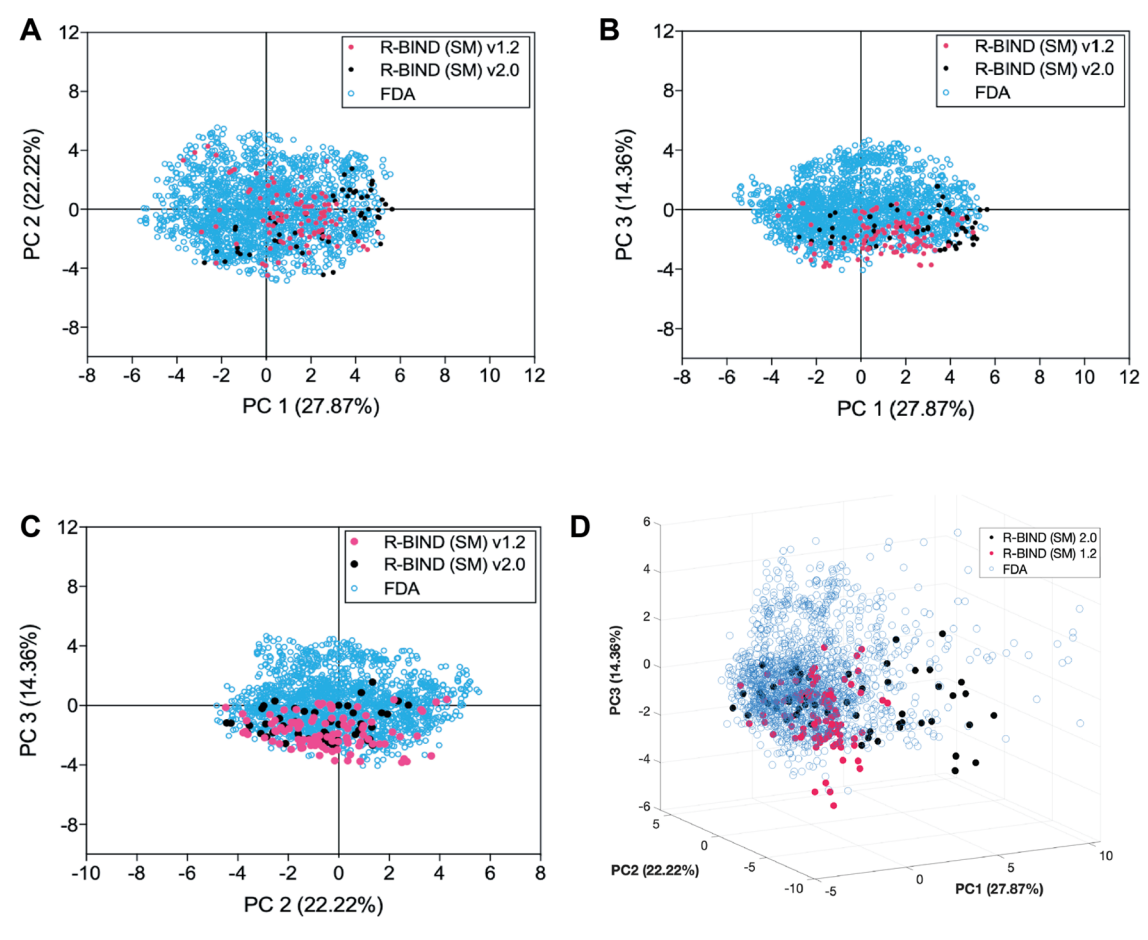


Figure 4. Principal component analysis (PCA) plots describing the variance between libraries. (A) Two-dimensional plot of principal components 1 and 2. (B) Two-dimensional plot of principal components 1 and 3. (C) Two-dimensional plot of principal components 2 and 3. (D) Three-dimensional plot of principal components 1, 2, and 3. R-BIND (SM) 2.0 includes only the new ligands between 1.2 and 2.0. Contributions of each parameter are listed in Table S9, and the loading plots for the first three principal components are shown in Figure S1.

due to reclassification and not a change in the chemical space itself.

To assess the 3D shapes of ligands, we conducted a PMI analysis that classified small molecule shapes as rod-, disc-, or sphere-like. We observed little to no differences between R-BIND (SM) 1.2 and R-BIND (SM) 2.0 updates, as assessed by the Kolmogorov–Smirnov test (Table S14), and both libraries remained enriched in rodlike shapes. Taken together, the generally minimal differences in the physicochemical and spatial properties, despite another increase in database size, further reinforced the notion that RNA-privileged chemical space exists and can be delineated.

R-BIND (SM) 2.0 vs FDA. Before comparing the newly updated R-BIND 2.0 (SM) library to FDA-approved small molecule drugs, our proxy for protein-targeting bioactive ligands, we conducted an update of the FDA library, as described in Supporting Information Section 1B. For all cheminformatic analyses, the FDA library used for comparison had an MW cutoff equal to the highest molecular weight ligand in the R-BIND (SM) 2.0 library (R-BIND (SM) 0132 A and B, 705.93 Da), in line with previous comparisons of these two libraries. In comparing the newly updated libraries, we again conducted a Mann—Whitney U analysis and found that 18 out of 20 physicochemical parameters between the FDA and R-BIND 2.0 library had statistically significant differences (Table S6). All structural and molecular recognition parameters that were previously found to be statistically significant between R-

BIND (SM) 1.2 and FDA followed the same trend in R-BIND (SM) 2.0 (Figure 3 and Tables S6 and S7). Some changes in the medicinal chemistry properties, as defined by Lipinski's³² and Veber's³³ rules, became statistically significant, though the averages do not violate the aforementioned druglike rules. Specifically, the properties such as the number of hydrogen bond acceptors became statistically significant (P-value = 0.010; Figure 3 and Table S6), while molecular weight and topological polar surface area became more statistically significant (P-value changed from 0.026 to <0.001 and from 0.002 to <0.001, respectively; Figure 3 and Tables S6 and S7). Given that the increase in the average molecular weight and surface area parameters was caused by R-BIND 2.0 ligand reclassification (see above; Tables S4 and S5), we generally attribute these differences to the addition of multivalent ligands. However, the observed increase in hydrogen bond acceptors but not hydrogen bond donors in R-BIND (SM) 2.0 regardless of the classification (Tables S4 and S5) suggests that this change may be a result of new R-BIND (SM) 2.0 ligands and could therefore represent a notable trend that will be tracked in future updates.

To visualize changes in the multidimensional chemical space between the FDA, R-BIND (SM) 1.2, and R-BIND (SM) 2.0, we utilized principal component analysis (PCA) as a dimension reduction technique. Notably, the R-BIND library remained in a subset of the space occupied by the FDA library (Figure 4). Several parameters strongly contributed to the first three principal components (Figure S1), which themselves only

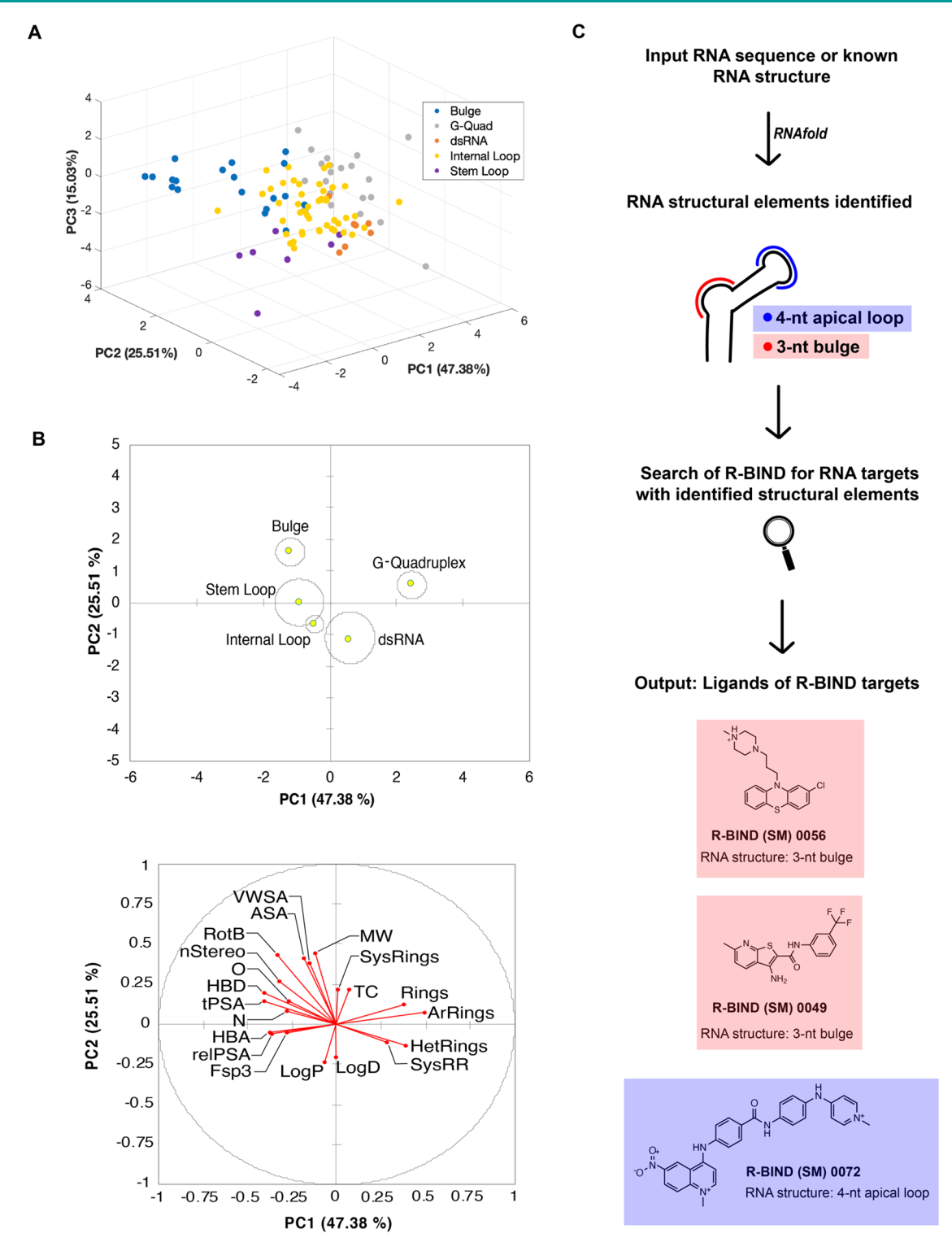


Figure 5. Analysis and implementation of RNA structure targeting using the R-BIND search tools. (A) Linear discriminant analysis (LDA) by RNA structure class explained by the first three principal components (PCs). (B) Two-dimensional centroid structures and associated loading plot with 20 physicochemical properties. Abbreviations are listed in Figure 3. (C) Workflow of newly implemented "RNA Structure Search" on the R-BIND website showing a theoretical input RNA containing a 3-nt bulge and 4-nt apical loop. Briefly, upon inputting a target RNA sequence with or without a dot-bracket notation, the RNAfold algorithm predicts the minimal free energy structure. The structure is inspected for bulge, internal loop, or apical loop structural elements of any size, which is then compared to the structural elements targeted by compounds in the database. The output represents all compounds in R-BIND that bind structures of the same size and motif.

explain 64% of the total variance (Figure 4D), supporting the need for such multidimensional analysis. An expansion of the R-BIND (SM) chemical space was observed as expected from the shifted cheminformatic parameters resulting from the reclassi-

fication, and indeed many of the ligands in this expanded space are those that moved from R-BIND (MV) 1.2 to R-BIND (SM) 2.0 (Figure S2). Further, a PCA analysis of R-BIND (SM) and (LM) 2.0 libraries showed unbiased clustering of the two

(Figure S3), with major contributors being MW, surface area, and lipophilicity parameters (Tables S10 and S11 and Figure S4). Lastly, R-BIND 2.0 ligands maintained significantly different enrichment in a rodlike character compared to the FDA library (Table S14).

Classification of RNA Target Structure-Ligand Pairs Reveals Differential Ligand Properties. With the notable increase in the number of ligands in R-BIND (SM) 2.0, we hypothesized that it might be possible to match the cheminformatic properties of ligands with their target RNA secondary or tertiary structures when known. This prospect would benefit the existing discovery strategy of rationally designing lead ligands based on RNA sequence and structure similarity. Indeed, Disney and co-workers have demonstrated that their database of RNA motif-small molecule interactions, Inforna,²⁵ which focuses on the affinity for select secondary structures such as loops and bulges, can serve to identify binders for targets such as micro-RNAs, viral RNAs, expanded repeat RNAs, and others.³⁴ Additionally, Zhang and co-workers have curated a database to explore RNA:ligand interactions by RNA structure, allowing for the identification of ligands across three databases that bind to RNA secondary structures while scoring the results based on sequence similarities between the input and reported RNA.24

We assessed the potential of our database to reveal novel determinants of structure-based selectivity in a bioactive setting for a comprehensive set of literature-reported ligands. Toward this end, linear discriminant analysis (LDA) was performed with the 20 cheminformatics parameters and classification of the SM ligands based on five RNA structural target classes (bulges, Gquadruplexes, double-stranded RNA, internal loops, and stem loops; Table S18). These classes were chosen because they each contained at least three ligands as well as ligands for at least three distinct RNA targets within that class, which we deemed as the minimum to obtain meaningful insights into a structural class. We found that the first three components explain ~88% of the variance within the predefined structure classes and showed significant separation (Figure 5A and Table S19). Smallmolecule properties such as rotatable bonds, surface area, and the number of ring systems had the greatest contribution to the variance (Figure S8). The separation was further validated through the training and cross-validation of the data set. In the training of the data set, around 84% of small molecules were correctly classified by the RNA structure motif that they target (Table S20). Furthermore, in the cross-validation, around 68% of small molecules were classified correctly (Table S21).

A closer look at two-dimensional centroids and the corresponding loading plot revealed several physicochemical properties that contributed to the structure classification (Figure 5B). For example, G-quadruplex-binding ligands have on average almost five rings and over four aromatic rings, the highest average number of rings and aromatic rings compared to all other structures examined (Table S22). Ligands that bind dsRNA were enriched in lipophilic character, while those that target more flexible and solvent-exposed bulges had a higher MW, number of rotatable bonds, and surface area parameters. Together, these results show the potential to use cheminformatics and RNA structural information in R-BIND to enrich for ligands targeting a given RNA secondary or tertiary structure.

Website Platform Contains Updated Nearest-Neighbor and Novel RNA Structure Search Algorithms. *Nearest-Neighbor Updates.* The change in the chemical space occupied by R-BIND (SM) 2.0 ligands granted an update

of the nearest-neighbor algorithm, which assesses if an input ligand exists in the RNA-privileged chemical space, as defined by the 20 physicochemical parameters. The average shortest Euclidean distance in this 20-dimensional space decreased from 2.0444 for R-BIND (SM) 1.2 to 1.7245 for R-BIND (SM) 2.0, suggesting that the distinct chemical space is becoming more populated.

RNA Structure Search Feature. To make the discovery of matching RNA structures with SM ligands of use to the community, we sought to incorporate a feature that enables parsing the database by the RNA secondary structure to find small molecules that target the same motif in the R-BIND website. We termed this feature "RNA Structure Search". Briefly, a user can input an RNA sequence or a defined secondary structure in the dot-bracket notation. After conducting a structure prediction embedded in the algorithm in the case that only the sequence is provided, the output will list the simple secondary structure motifs found (bulge, apical loop, or internal loop), all small molecules that bind motifs of the same size (e.g., 2-nt bulge), and the sequences of the secondary structure elements that the R-BIND ligands bind (Figure 5C). We note that the embedded feature of predicting the secondary structure based on input sequence takes into account only the lowest energy structure, as analyzed by RNAfold. It is well known that alternative or less-populated structures may exist in the dynamic ensemble of an RNA target of interest and that environmental factors such as temperature and salt concentrations should be considered when assessing the accuracy of the predicted RNA structure. 35-37 In the future, we plan on incorporating features in which these factors can be controlled, in addition to predicting the likelihood of forming more complex structures such as G-quadruplexes. In casting a wide net with the RNA structure search and identifying all molecules that have been reported to bind a broad set of secondary structure motifs, the promise of RNA-targeting ligands will be a possibility for many therapeutically relevant RNA structures.

CONCLUSIONS

While once considered undruggable, RNA molecules are gaining increased consideration as tractable and sometimes even advantageous targets in diseases compared to traditionally targeted proteins.9 Timely identification of trends in RNAsmall molecule discovery, screening approaches, and RNAprivileged chemotypes along with tool development to apply these findings holds great promise in advancing the field. In this work, we demonstrate that updating the R-BIND database continues to provide insights into the progress and novel strategies employed in the RNA-targeting community. We find that the field still embraces focused screens as a screening strategy while introducing innovative high-throughput assays as well as in vivo discovery studies. Further, notable progress has been made in terms of both new targets such as long noncoding RNAs and the disease phenotypes modulated such as those in Huntington's disease and fungal infections. Together, insights gained from R-BIND 2.0 confirm that significant progress has been made in the field and that this trend will continue for years to come.

The analysis of potential changes in the physicochemical and spatial properties of ligands in the database continues to define and analyze RNA-privileged chemical space to aid future work. In the R-BIND 2.0 update, the addition of new ligands did not change the unique physicochemical properties or rodlike shape preferences found in RNA-targeting small molecules compared

to protein-binding ligands. This further supports the hypothesis of the existence of a unique RNA-targeting chemical space. In addition, the increase in library size allowed for insights into the physicochemical properties that may distinguish ligands that target specific RNA secondary structures. With advances in pattern recognition³⁸- and machine learning³⁹-based applications in small molecule modulation of RNA structure, the emergence of initial predictive parameters for structural classes analyzed herein represents an exciting new direction for the field and one that we will continue to explore. One immediate direction is the incorporation of additional cheminformatics parameters such as those used in our recent work for establishing quantitative structure—activity relationships.⁴⁰

To increase the utility of the database website and additionally benefit researchers, the website has been updated to incorporate more search features. The new "RNA Structure Search" includes the ability to input an RNA target of interest and parse the database for similar RNA structural elements. During the preparation of this manuscript, a database termed "RNA Ligands" from Zhang and co-workers was published,² consisting of R-BIND 1.2, Inforna, and PDB RNA:ligand pairs and offering similar RNA structure-based analyses, highlighting the interest in the field to better understand and explore interactions based on RNA target structures. We note, however, that the structure search implemented herein directly queries the R-BIND 2.0 database for bulges, internal loops, and apical loops, which were verified as the secondary structures with enough ligands in the database to yield meaningful results. We are confident that these resources can expedite the structure-guided rational design of small molecules and aid the exploration of novel RNA targets, including those recently identified in SARS-CoV-2.^{24,41,42} Future R-BIND updates and the concurrent increase in RNA structural information will enable synergistic insights that will propel the RNA-targeting field to new heights.

METHODS

Cheminformatics Calculations. The noncorrected (NC) SMILES strings for all R-BIND ligands were batch-processed and corrected to their major protonation and tautomer state (pH = 7.4) with ChemAxon calculator plugins (20.8.2). Next, the 20 cheminformatic parameters were calculated using ChemAxon Chemical Terms Evaluator (Marvin 20.8.2, 2020, http://www.chemaxon.com). To compare different libraries, independent two-group Mann—Whitney U tests were performed in R software (4.0.0, 2020). The rationale for the selection of cheminformatic parameters, as well as the descriptions and chemical term evaluator expressions for all 20 parameters, was previously published. 16,22

Principal Component Analysis (PCA). All 20 cheminformatic parameters were normalized to the average and standard deviation of the libraries analyzed, as described previously. ¹⁶ The normalized data was used to perform principal component analysis (PCA) in XLSTAT-Student (version 2019.3.2.61793).

Principal Moments of Inertia (PMI) Analysis. Calculations were conducted, as described previously, ¹⁶ for the R-BIND (SM) v1.2, R-BIND (SM) v2.0, and the FDA 2020 library with the molecular weight restriction (n=1834). Protonation- and tautomer-corrected SMILES codes from SI Section 3 were utilized for all libraries. Specifically, the Molecular Operating Environment software was used (MOE, version 2019.01) to set up a conformational search utilizing input parameters listed in Table S12, using a stochastic method with the MMFF94 force field and generalized Born solvation model. The following options were checked: calculate force field partial charges and hydrogens. The normalized (npr1 and npr2) PMI vectors were calculated for each conformation after the search was complete, and the values were Boltzmann-averaged to result in a single coordinate. Details regarding the energy window rationale and Boltzmann average calculation were

previously published. ¹⁶ The triangular graph shown in Figure S5 was constructed by plotting the resulting npr1 and npr2 coordinates as vertices of rod- (0,1), sphere- (1,1), and disc-like (0.5,0.5) shapes. The Euclidean distance of each ligand coordinate to each vertex was calculated and ordered from smallest to largest to plot cumulative distance distributions (Figure S6). A two-sided, two-sample Kolmogorov–Smirnov test was conducted to assess the statistical significance of the plotted differences using R statistical software v.3.4.3 (2017), and the results are listed in Table S14. To analyze the shape populations of the libraries, the large triangular plot was partitioned into 4 (Table S15) or 16 (Table S16) equal-sized subtriangles using cell-based partitioning. The triangle partition figures and script details were previously published. ^{16,22}

Linear Discriminant Analysis (LDA). All 20 cheminformatic parameters were used to perform linear discriminant analysis (LDA) in XLSTAT-Student (version 2019.3.2.61793). Only RNA structure classes with five or more ligands in R-BIND (SM) 2.0 were included in the LDA analysis (internal loop, bulge, stem loop, g-quadruplex, and dsRNA).

RNA Structure Search Algorithm. The in-house-written Python algorithm (version 3.7.4) was made to search the unique secondary structure(s) in the user-input connecting (.ct) file and outputs R-BIND ligands that target the detected secondary structure(s). Details on the algorithm construction rationale and its stepwise workflow can be found in SI Section 7 and Figure S9.

ASSOCIATED CONTENT

Supporting Information

The Supporting Information is available free of charge at https://pubs.acs.org/doi/10.1021/acschembio.2c00224.

Overview, target, quantitative data, design, and discovery, as well as primary literature sources for R-BIND v2.0 (RBIND v2.0 A.xlsx) (xlsx)

Qualitative data for R-BIND v2.0 containing experimental details for in vitro assays, cell-based assays, and/or animal model studies conducted after the primary screen for each ligand (RBIND v2.0 B.xlsx) (xlsx)

Supporting tables, supporting figures, and additional details regarding R-BIND v2.0 database curation, content, computational methods, and RNA structure algorithm (PDF)

AUTHOR INFORMATION

Corresponding Authors

Blanton S. Tolbert — Department of Chemistry, Case Western Reserve University, Cleveland, Ohio 441106, United States; orcid.org/0000-0003-2456-0443; Email: bst18@case.edu

Amanda E. Hargrove — Department of Chemistry, Duke University, Durham, North Carolina 27705, United States; orcid.org/0000-0003-1536-6753;

Email: amanda.hargrove@duke.edu

Authors

Anita Donlic – Department of Chemical and Biological Engineering, Princeton University, Princeton, New Jersey 08540, United States

Emily G. Swanson – Department of Chemistry, Duke University, Durham, North Carolina 27705, United States

Liang-Yuan Chiu – Department of Chemistry, Case Western Reserve University, Cleveland, Ohio 441106, United States

Sarah L. Wicks – Department of Chemistry, Duke University, Durham, North Carolina 27705, United States

Aline Umuhire Juru — Department of Chemistry, Duke University, Durham, North Carolina 27705, United States

- Zhengguo Cai Department of Chemistry, Duke University, Durham, North Carolina 27705, United States
- Kamillah Kassam Department of Chemistry, Duke University, Durham, North Carolina 27705, United States
- Chris Laudeman Department of Chemistry, Duke University, Durham, North Carolina 27705, United States
- Bilva G. Sanaba Department of Chemistry, Duke University, Durham, North Carolina 27705, United States
- Andrew Sugarman Department of Chemistry, Case Western Reserve University, Cleveland, Ohio 441106, United States
- Eunseong Han Department of Chemistry, Duke University, Durham, North Carolina 27705, United States

Complete contact information is available at: https://pubs.acs.org/10.1021/acschembio.2c00224

Author Contributions

A.D. and E.G.S. contributed equally. Conceptualization: A.E.H., B.S.T., and A.D.; database curation and data collection: A.D., E.G.S., S.L.W., A.U.J., Z.C., K.K., and C.L.; cheminformatics, principal moments of inertia, principal component, linear discriminant, and nearest-neighbor analyses: E.G.S., S.L.W., and Z.C.; RNA structure search algorithm: L.-Y.C. and A.A.K.; website integration: B.G.S. and E.H.; supervision: A.E.H. and B.S.T.; writing (original draft): A.D., E.G.S., and A.E.H; and manuscript editing: all.

Funding

Duke University authors (A.E.H., A.D., E.G.S., S.L.W., A.U.J., Z.C., K.K., C.L., and E.H.) were supported by a combination of Duke University funds, the U.S. National Institutes of Health (R35GM124785, U54 AI150470), NSF (CAREER 1750375), and the Alfred P. Sloan Foundation. B.S.T., L.-Y.C., and A.S. were supported by NIH R01 GM126833 and AI150830.

Notes

The authors declare no competing financial interest.

ACKNOWLEDGMENTS

The authors are grateful to the members of Hargrove and Tolbert labs for helpful discussions. The authors thank W. Day and M. Peterson for essential assistance and help with R-BIND website maintenance and addition of new features. TOC graphic was made with BioRender.

REFERENCES

- (1) Slaby, O.; Laga, R.; Sedlacek, O. Therapeutic targeting of noncoding RNAs in cancer. *Biochem. J.* 2017, 474, 4219–4251.
- (2) Bernat, V.; Disney, M. D. RNA Structures as Mediators of Neurological Diseases and as Drug Targets. *Neuron* **2015**, *87*, 28–46.
- (3) Tang, R.; Long, T.; Lui, K. O.; Chen, Y.; Huang, Z. P. A Roadmap for Fixing the Heart: RNA Regulatory Networks in Cardiac Disease. *Mol. Ther.*–*Nucleic Acids* **2020**, 20, 673–686.
- (4) McKnight, K. L.; Heinz, B. A. RNA as a target for developing antivirals. *Antiviral Chem. Chemother.* **2003**, *14*, 61–73.
- (5) Hong, W.; Zeng, J.; Xie, J. Antibiotic drugs targeting bacterial RNAs. *Acta Pharm. Sin. B* **2014**, *4*, 258–265.
- (6) Fedorova, O.; Jagdmann, G. E.; Adams, R. L.; Yuan, L.; Van Zandt, M. C.; Pyle, A. M. Small molecules that target group II introns are potent antifungal agents. *Nat. Chem. Biol.* **2018**, *14*, 1073–1078.
- (7) Connelly, C. M.; Moon, M. H.; Schneekloth, J. S. The Emerging Role of RNA as a Therapeutic Target for Small Molecules. *Cell Chem. Biol.* **2016**, *23*, 1077–1090.
- (8) Di Giorgio, A.; Duca, M. Synthetic small molecule RNA ligands: future prospects as therapeutic agents. *Medchemcomm* **2019**, *10*, 1242–1255.

- (9) Donlic, A.; Hargrove, A. E. Targeting RNA in mammalian systems with small molecules. *Wiley Interdiscip. Rev.: RNA* **2018**, *9*, No. e1477.
- (10) Hermann, T. Small molecules targeting viral RNA. Wiley Interdiscip. Rev. 2016, 7, 726–743.
- (11) Meyer, S. M.; Williams, C. C.; Akahori, Y.; Tanaka, T.; Aikawa, H.; Tong, Y.; Childs-Disney, J. L.; Disney, M. D. Small molecule recognition of disease-relevant RNA structures. *Chem. Soc. Rev.* **2020**, 49, 7167–7199.
- (12) Warner, K. D.; Hajdin, C. E.; Weeks, K. M. Principles for targeting RNA with drug-like small molecules. *Nat. Rev. Drug Discovery* **2018**, *17*, 547–558.
- (13) Rizvi, N. F.; Smith, G. F. RNA as a small molecule druggable target. *Bioorg. Med. Chem. Lett.* **2017**, *27*, 5083–5088.
- (14) Genentech (2020)FDA approves Genentech's Evrysdi (risdiplam) for treatment of spinal muscular atrophy (SMA) in adults and children 2 months and older. https://www.gene.com/media/pressreleases/14866/2020-08-07/fda-approves-genentechs-evrysdirisdipla(accessed January 29, 2022).
- (15) Cech, T. R.; Steitz, J. A. The noncoding RNA revolution-trashing old rules to forge new ones. *Cell* **2014**, *157*, 77–94.
- (16) Morgan, B. S.; Forte, J. E.; Culver, R. N.; Zhang, Y.; Hargrove, A. E. Discovery of Key Physicochemical, Structural, and Spatial Properties of RNA-Targeted Bioactive Ligands. *Angew. Chem., Int. Ed.* **2017**, *56*, 13498–13502.
- (17) Morgan, B. S.; Forte, J. E.; Hargrove, A. E. Insights into the development of chemical probes for RNA. *Nucleic Acids Res.* **2018**, *46*, 8025–8037.
- (18) Haniff, H. S.; Knerr, L.; Liu, X.; Crynen, G.; Boström, J.; Abegg, D.; Adibekian, A.; Lekah, E.; Wang, K. W.; Cameron, M. D.; et al. Design of a small molecule that stimulates vascular endothelial growth factor A enabled by screening RNA fold-small molecule interactions. *Nat. Chem.* **2020**, *12*, 952–961.
- (19) Rizvi, N. F.; Santa Maria, J. P.; Nahvi, A.; Klappenbach, J.; Klein, D. J.; Curran, P. J.; Richards, M. P.; Chamberlin, C.; Saradjian, P.; Burchard, J.; et al. Targeting RNA with Small Molecules: Identification of Selective, RNA-Binding Small Molecules Occupying Drug-Like Chemical Space. *SLAS Discovery* **2020**, *25*, 384–396.
- (20) Hewitt, W. M.; Calabrese, D. R.; Schneekloth, J. S. Evidence for ligandable sites in structured RNA throughout the Protein Data Bank. *Bioorg. Med. Chem.* **2019**, *27*, 2253–2260.
- (21) Padroni, G.; Patwardhan, N. N.; Schapira, M.; Hargrove, A. E. Systematic analysis of the interactions driving small molecule-RNA recognition. *RSC Med. Chem.* **2020**, *11*, 802–813.
- (22) Morgan, B. S.; Sanaba, B. G.; Donlic, A.; Karloff, D. B.; Forte, J. E.; Zhang, Y.; Hargrove, A. E. R-BIND: An Interactive Database for Exploring and Developing RNA-Targeted Chemical Probes. *ACS Chem. Biol.* **2019**, *14*, 2691–2700.
- (23) Wehler, T. Structure-Based Discovery of Small Molecules Binding to RNA, Brenk, R., Ed.; RNA Therapeutics, 2018; pp 47–77.
- (24) Sun, S.; Yang, J.; Zhang, Z. RNALigands: a database and web server for RNA ligand interactions. RNA 2022, 28, 115–122.
- (25) Disney, M. D.; Winkelsas, A. M.; Velagapudi, S. P.; Southern, M.; Fallahi, M.; Childs-Disney, J. L. Inforna 2.0: A Platform for the Sequence-Based Design of Small Molecules Targeting Structured RNAs. ACS Chem. Biol. 2016, 11, 1720–1728.
- (26) Chan, H. Y. E.; Ngo, J.C.-K.; Wong, C.-H.; Zhang, Q.; Shaohong, P. Small molecule inhibitors targeting CAG-repeat RNA toxicity in polyglutamine diseases. US10143666B22015.
- (27) Abulwerdi, F. A.; Xu, W.; Ageeli, A. A.; Yonkunas, M. J.; Arun, G.; Nam, H.; Schneekloth, J. S.; Dayie, T. K.; Spector, D.; Baird, N.; Le Grice, S. F. J. Selective Small-Molecule Targeting of a Triple Helix Encoded by the Long Noncoding RNA, MALAT1. ACS Chem. Biol. 2019, 14, 223–235.
- (28) Ren, Y.; Wang, Y. F.; Zhang, J.; Wang, Q. X.; Han, L.; Mei, M.; Kang, C. S. Targeted design and identification of AC1NOD4Q to block activity of HOTAIR by abrogating the scaffold interaction with EZH2. Clin. Epigenet. 2019, 11, No. 29.
- (29) Matarlo, J. S.; Krumpe, L. R. H.; Heinz, W. F.; Oh, D.; Shenoy, S. R.; Thomas, C. L.; Goncharova, E. I.; Lockett, S. J.; O'Keefe, B. R. The

Natural Product Butylcycloheptyl Prodiginine Binds Pre-miR-21, Inhibits Dicer-Mediated Processing of Pre-miR-21, and Blocks Cellular Proliferation. *Cell Chem. Biol.* **2019**, *26*, 1133–1142.e4.

- (30) Vicens, Q.; Mondragón, E.; Reyes, F. E.; Coish, P.; Aristoff, P.; Berman, J.; Kaur, H.; Kells, K. W.; Wickens, P.; Wilson, J.; et al. Structure-Activity Relationship of Flavin Analogues That Target the Flavin Mononucleotide Riboswitch. *ACS Chem. Biol.* **2018**, *13*, 2908–2919.
- (31) Campagne, S.; Boigner, S.; Rüdisser, S.; Moursy, A.; Gillioz, L.; Knörlein, A.; Hall, J.; Ratni, H.; Cléry, A.; Allain, F. H. Structural basis of a small molecule targeting RNA for a specific splicing correction. *Nat Chem. Biol.* **2019**, *15*, 1191–1198.
- (32) Lipinski, C. A.; Lombardo, F.; Dominy, B. W.; Feeney, P. J. Experimental and computational approaches to estimate solubility and permeability in drug discovery and development settings. *Adv. Drug Delivery Rev.* **2001**, *46*, 3–26.
- (33) Veber, D. F.; Johnson, S. R.; Cheng, H. Y.; Smith, B. R.; Ward, K. W.; Kopple, K. D. Molecular properties that influence the oral bioavailability of drug candidates. *J. Med. Chem.* **2002**, *45*, 2615–2623.
- (34) Ursu, A.; Childs-Disney, J. L.; Andrews, R. J.; O'Leary, C. A.; Meyer, S. M.; Angelbello, A. J.; Moss, W. N.; Disney, M. D. Design of small molecules targeting RNA structure from sequence. *Chem. Soc. Rev.* **2020**, *49*, 7252–7270.
- (35) Ganser, L. R.; Kelly, M. L.; Herschlag, D.; Al-Hashimi, H. M. The roles of structural dynamics in the cellular functions of RNAs. *Nat. Rev. Mol. Cell Biol.* **2019**, 20, 474–489.
- (36) Wu, M.-P.; D'Souza, V. Alternate RNA Structures. Cold Spring Harbor Perspect. Biol. 2020, 12, No. a032425.
- (37) Eubanks, C. S.; Hargrove, A. E. Sensing the impact of environment on small molecule differentiation of RNA sequences. *Chem. Commun.* **2017**, 53, 13363–13366.
- (38) Eubanks, C. S.; Hargrove, A. E. RNA Structural Differentiation: Opportunities with Pattern Recognition. *Biochemistry* **2019**, *58*, 199–213.
- (39) Oliver, C.; Mallet, V.; Gendron, R. S.; Reinharz, V.; Hamilton, W. L.; Moitessier, N.; Waldispühl, J. Augmented base pairing networks encode RNA-small molecule binding preferences. *Nucleic Acids Res.* **2020**, *48*, 7690–7699.
- (40) Patwardhan, N. N.; Cai, Z.; Umuhire Juru, A.; Hargrove, A. E. Driving factors in amiloride recognition of HIV RNA targets. *Org. Biomol. Chem.* **2019**, *17*, 9313–9320.
- (41) Manfredonia, I.; Nithin, C.; Ponce-Salvatierra, A.; Ghosh, P.; Wirecki, T. K.; Marinus, T.; Ogando, N. S.; Snijder, E. J.; van Hemert, M. J.; Bujnicki, J. M.; Incarnato, D. Genome-wide mapping of SARS-CoV-2 RNA structures identifies therapeutically-relevant elements. *Nucleic Acids Res.* **2020**, *48*, 12436–12452.
- (42) Zafferani, M.; Haddad, C.; Luo, L.; Davila-Calderon, J.; Chiu, L.-Y.; Mugisha, C. S.; Monaghan, A. G.; Kennedy, A. A.; Yesselman, J. D.; Gifford, R. J.; et al. Amilorides inhibit SARS-CoV-2 replication in vitro by targeting RNA structures. *Sci. Adv.* **2021**, *7*, No. eabl6096.

□ Recommended by ACS

Quantitative Structure–Activity Relationship (QSAR) Study Predicts Small-Molecule Binding to RNA Structure

Zhengguo Cai, Amanda E. Hargrove, et al.

MAY 06, 2022

JOURNAL OF MEDICINAL CHEMISTRY

READ 🗹

RNAPosers: Machine Learning Classifiers for Ribonucleic Acid-Ligand Poses

Sahil Chhabra, Aaron T. Frank, et al.

MAY 19, 2020

THE JOURNAL OF PHYSICAL CHEMISTRY B

READ 🗹

Efficient NMR Screening Approach to Discover Small Molecule Fragments Binding Structured RNA

Matthew D. Shortridge and Gabriele Varani

JULY 13, 2021

ACS MEDICINAL CHEMISTRY LETTERS

READ 🗹

Protein-RNA Docking Using ICM

Yelena A. Arnautova, Maxim Totrov, et al.

JULY 17, 2018

JOURNAL OF CHEMICAL THEORY AND COMPUTATION

READ **C**

Get More Suggestions >